



Published in final edited form as:

*Circ Arrhythm Electrophysiol.* 2017 April ; 10(4): . doi:10.1161/CIRCEP.115.003560.

## Azithromycin Causes a Novel Proarrhythmic Syndrome

Zhenjiang Yang, MD, PhD, Joseph K. Prinsen, DO, PhD, Kevin R. Bersell, PhD, Wangzhen Shen, MD, Liudmila Yermalitskaya, PhD, Tatiana Sidorova, PhD, Paula B. Luis, PhD, Lynn Hall, BA, Wei Zhang, MS, Liping Du, PhD, Ginger Milne, PhD, Patrick Tucker, PhD, Alfred L. George Jr., MD\*, Courtney M. Campbell, MD, PhD, Robert A. Pickett, MD, Christian M. Shaffer, BS, Nagesh Chopra, MD, Tao Yang, MD, PhD, Bjorn C. Knollmann, MD, PhD, Dan M. Roden, MD, and Katherine T. Murray, MD

Departments of Medicine and Pharmacology, Vanderbilt University School of Medicine, Nashville, TN

### Abstract

**Background**—The widely-used macrolide antibiotic azithromycin increases risk of cardiovascular and sudden cardiac death, although the underlying mechanisms are unclear. Case reports, including the one we document here, demonstrate that azithromycin can cause rapid, polymorphic ventricular tachycardia in the absence of QT prolongation, indicating a novel proarrhythmic syndrome. We investigated the electrophysiologic effects of azithromycin *in vivo* and *in vitro* using mice, cardiomyocytes, and human ion channels heterologously expressed in human embryonic kidney (HEK 293) and Chinese hamster ovary (CHO) cells.

**Methods and Results**—In conscious telemetered mice, acute intraperitoneal and oral administration of azithromycin caused effects consistent with multi-ion channel block, with significant sinus slowing and increased PR, QRS, QT, and QTc intervals, as seen with azithromycin overdose. Similarly, in HL-1 cardiomyocytes, the drug slowed sinus automaticity, reduced phase 0 upstroke slope, and prolonged action potential duration. Acute exposure to azithromycin reduced peak SCN5A currents in HEK cells ( $IC_{50}=110\pm 3\mu M$ ) and  $Na^+$  current in mouse ventricular myocytes. However, with chronic (24hour) exposure, azithromycin caused a ~2-fold increase in both peak and late SCN5A currents, with findings confirmed for  $I_{Na}$  in cardiomyocytes. Mild block occurred for  $K^+$  currents representing  $I_{Kr}$  (CHO cells expressing hERG;  $IC_{50}=219\pm 21\mu M$ ) and  $I_{Ks}$  (CHO cells expressing KCNQ1+KCNE1;  $IC_{50}=184\pm 12\mu M$ ), while azithromycin suppressed L-type  $Ca^{++}$  currents (rabbit ventricular myocytes;  $IC_{50}=66.5\pm 4\mu M$ ) and  $I_{K1}$  (HEK cells expressing Kir2.1;  $IC_{50}=44\pm 3\mu M$ ).

**Conclusions**—Chronic exposure to azithromycin increases cardiac  $Na^+$  current to promote intracellular  $Na^+$  loading, providing a potential mechanistic basis for the novel form of proarrhythmia seen with this macrolide antibiotic.

Correspondence: Dr. Katherine T. Murray, Division of Clinical Pharmacology, Room 559 Preston Research Building, Vanderbilt University School of Medicine, 2220 Pierce Avenue, Nashville, TN 37232-6602, Tel: (615) 936-3420, Fax: (615) 936-2746, kathy.murray@vanderbilt.edu.

\*Current affiliation: Department of Pharmacology, Northwestern University Feinberg School of Medicine, Chicago, IL

**Disclosures:** none

## Keywords

sodium channels; calcium channel; potassium channels; pharmacology; mouse; azithromycin; proarrhythmia; HL-1 cells

## Journal Subject Terms

Arrhythmias; Ion Channels/Membrane Transport; Electrophysiology; Basic Science Research; Translational Studies

---

## Introduction

Sudden cardiac death due to non-cardiac medications is a major public health issue, in particular given its preventable nature. The scope of this problem is illustrated by the fact that drug-related proarrhythmia has been most common cause for removal of medications from the US market in recent decades.<sup>1</sup> An improved understanding of the basic mechanisms causing drug-related sudden cardiac death would lead to safer pharmacotherapy.

The macrolide antibiotics erythromycin and clarithromycin are associated with increased risk of serious ventricular tachyarrhythmias and sudden cardiac death, while azithromycin was long considered to have minimal adverse cardiac effects.<sup>2</sup> However, because of occasional case reports of marked QT prolongation and/or serious ventricular arrhythmias, as well as concerning data from the FDA AERS,<sup>3-10</sup> we previously conducted a retrospective cohort study to examine azithromycin safety.<sup>11</sup> We found that azithromycin users had an increased risk of cardiovascular mortality and sudden cardiac death, compared to users of amoxicillin.

Several mechanisms have been described whereby drugs can increase susceptibility to serious ventricular tachyarrhythmias and sudden cardiac death, analogous to inherited arrhythmia syndromes. First, a reduction in cardiac  $\text{Na}^+$  current ( $I_{\text{Na}}$ ) can lead to slowed conduction, facilitating reentrant ventricular arrhythmias.<sup>12, 13</sup> This likely accounts for increased mortality in patients with coronary artery disease treated with  $\text{Na}^+$  channel blockers, and in the Brugada syndrome, where  $\text{Na}^+$  current is down-regulated. In the setting of overdose and IV administration,<sup>14, 15</sup> azithromycin can cause QRS widening suggesting  $I_{\text{Na}}$  block, but this has not been reported during oral dosing. Second, excessive prolongation of ventricular repolarization promotes abnormal triggered activity in the form of early afterdepolarizations (EADs) and ultimately torsades de pointes.<sup>16</sup> QT prolongation occurs with either reduced outward or increased inward currents, and it accounts for the increased risk associated with  $\text{K}^+$  channel-blocking antiarrhythmic drugs,<sup>17, 18</sup> as well as the congenital long QT syndrome.<sup>19</sup> Reports indicate that the incidence of drug-induced long QT syndrome with azithromycin is less than that seen with the older macrolides, and that torsades de pointes is unusual. Third, patients can develop polymorphic ventricular tachyarrhythmias in the setting of a normal QT interval,<sup>13, 20, 21</sup> exemplified by bidirectional ventricular tachycardia that can occur with digitalis therapy. Digoxin-mediated inhibition of the  $\text{Na}^+$ - $\text{K}^+$  ATPase causes intracellular  $\text{Na}^+$  loading, disrupting intracellular  $\text{Ca}^{++}$

homeostasis via reverse mode  $\text{Na}^+\text{-Ca}^{++}$  exchange, with increased intracellular  $\text{Ca}^{++}$  causing delayed afterdepolarizations (DADs) and ventricular tachycardia (VT). Similarly, spontaneous  $\text{Ca}^{++}$  release from the sarcoplasmic reticulum (SR) during catecholaminergic polymorphic ventricular tachycardia (CPVT) results in polymorphic VT in the absence of QT prolongation.

A prior case report suggested that azithromycin could cause a distinct, previously-undescribed type of drug-induced proarrhythmia, manifested by rapid polymorphic VT in the absence of ECG or structural abnormalities: specifically the QT was normal, with no pause prior to the tachycardia.<sup>6</sup> We describe a similar case and together, these data imply a novel proarrhythmic mechanism. Accordingly, we examined the electrophysiologic effects of azithromycin *in vivo* and *in vitro* to investigate the molecular basis for this unusual form of drug-mediated proarrhythmia.

## Materials and Methods

### Reagents

Azithromycin was provided by Pfizer Inc. (Groton, CT) and dissolved in dimethyl sulfoxide to generate a 100mM stock solution (stored at  $-20^\circ\text{C}$ ). The stock solution was serially diluted in bath solution to the final concentrations prior to each experiment. The drug was prepared for oral administration as described previously.<sup>22</sup>

### Cell Preparations

The effects of azithromycin on the ionic currents under study were investigated using heterologously-expressed human channels as well as cardiomyocytes. For cardiomyocyte studies, the species selected for experimentation was one that would optimize recording conditions for the specific current under study.

Human embryonic kidney (HEK 293) cells that stably expressed either human KCNH2 (hERG) or human SCN5A were kindly provided by Dr. Craig January (University of Wisconsin) and Dr. Alfred George (Northwestern University), respectively. A Chinese hamster ovary (CHO) cell line stably expressing KCNQ1 and KCNE1 to generate  $\text{I}_{\text{K}_S}$  currents was also provided by Dr. George. The construct encoding the human Kir2.1 channel was kindly provided by Dr. Antonin Lapoli, with transient transfection in HEK cells as reported previously.<sup>23, 24</sup> HEK293, CHO, and HL-1 cells were cultured as described.<sup>23, 25–28</sup>

Isolation of rabbit ventricular myocytes was performed using the method of Bassani<sup>29</sup> with minor modifications. Murine left ventricular myocytes were prepared from 10 to 12-week-old male mice as previously described.<sup>30</sup> The investigation conforms with the Guide for the Care and Use of Laboratory Animals published by the US National Institutes of Health (NIH Publication No. 85-23, revised 1996).

### Data Acquisition

**Mouse ECGs**—A DSI (Data Science International, St. Paul, MN) telemetry system was used to monitor and collect ECG data from conscious, freely moving laboratory mice. C57BL/6 mice (age 10–12 weeks) were anesthetized using Ketamine 100  $\mu\text{g}/\text{g}$  and Xylazine

10 $\mu$ g/g injected intraperitoneally (IP) to place a radio transmitter (EA-F20) in the abdominal cavity. The mouse ECG telemetry system contains two electrical ECG leads connected to a radio transmitter with subcutaneous electrodes in lead I configuration. Upon activation of the transmitter by a magnet, the electrical signals were transmitted wirelessly to a nearby receiver (RPC-1) attached to an amplifier (MX2) and computer system for data acquisition (Ponemah v6.10, sampling frequency 2 KHz), storage and analysis. Animals were allowed to recover for at least 5 days after surgery prior to experimentation. Each mouse served as its own control with resting ECG recorded for at least 15–30 minutes prior to any intervention. For IP administration, azithromycin 50mg/kg was injected, followed by 100mg/kg IP one hour later. ECG monitoring continued for at least one hour after the second injection. A separate group of mice were treated with oral azithromycin for 3 days, using a dose that was efficacious in treating infections.<sup>31</sup> Baseline ECG was recorded, azithromycin 50mg/kg was administered by oral gavage, and the ECG was recorded for 2h. This was repeated for 2 or 3 additional days.

**Action potentials**—Spontaneous action potentials were recorded at 37°C from HL-1 cells as previously described (Data Supplement).<sup>28</sup> Cells chosen for experimentation had a resting membrane potential of at least –55mV, overshoot exceeding 20mV, regular rhythmicity, and a stable spontaneous cycle length for at least 5 min.

**Ionic currents**—All currents were recorded at room temperature (22 $\pm$ 1°C) in the whole-cell configuration with an Axopatch-200B amplifier (Molecular Devices, Sunnyvale, CA). Currents were low-pass filtered at 5 kHz and digitized with a DigiData 1320A. Capacitance and 80–95% series resistance were routinely compensated. Leak subtraction was completed using user-specified after-the fact-leakage correction of pCLAMP. Na<sup>+</sup> current, rapidly ( $I_{Kr}$ ) and slowly-activating ( $I_{Ks}$ ) delayed rectifier K<sup>+</sup> currents, L- and T-type Ca<sup>2+</sup> currents, and inward rectifier current ( $I_{K1}$ ) were recorded as detailed in the Data Supplement. Pipettes were pulled (Sutter Instrument, Novato, CA) using Borosilicate glass having tip resistances of 0.5 to 1 M $\Omega$ .

**Pulse protocols and solutions**—These are described in the Data Supplement and illustrated in the representative figures.

## Data analysis

**ECG data**—Mouse ECG waveforms over a 10 sec period were averaged to obtain measurements of the RR, PR, QRS, QT, and QTc intervals and heart rate using LabChart (version 8.1.5, AD Instruments, Colorado Springs, CO) and are presented as mean  $\pm$  SEM. QTc was calculated using the normalized Bazett formula ( $QTc = QT/[RR/100]^{1/2}$ ).<sup>32</sup>

**Action potentials and ionic currents**—Data were analyzed using Clampfit 10.4 software (Molecular Devices, Sunnyvale, CA), Excel 2010 (Microsoft, Redmond, WA), and Origin 9.0 (OriginLab Corporation, Northampton, MA), with action potential measurements obtained as previously described (Data Supplement).<sup>7</sup> Current amplitudes were normalized by cell capacitance and expressed as current density. All activation and inactivation curves were fitted with a single Boltzmann function as follows:  $y = A2 + (A1 - A2) / (1 + \exp((V_m -$

$V_{1/2}/k$ ) where  $A_1$  is maximum current,  $A_2$  is the minimum current,  $V_{1/2}$  is the half-activation potential or half-inactivation potential (i.e., half availability),  $V_m$  is test voltage, and  $k$  is slope factor. Fractional blockade was defined as follows:  $f=1-I_{drug}/I_{con}$ , where  $I_{con}$  and  $I_{drug}$  are current amplitudes in the absence and presence of azithromycin, respectively. Dose-response curves were fit by the equation:  $y = B_1 + (B_2 - B_1) / (1 + 10^{(\log x - x_0) * p})$ , where  $B_1$  is the bottom asymptote,  $B_2$  is the top asymptote,  $\log x_0$  is  $IC_{50}$ ,  $x$  is azithromycin concentration, and  $p$  is hill slope.

### Whole Exome Sequencing

After informed consent, DNA was extracted from peripheral blood leukocytes and protein coding regions targeted using the Agilent SureSelect All Exon V3 capture kit. High throughput DNA sequencing was then performed using the Illumina HiSeq 2500 instrument with the paired-end sequencing protocol generating just under 100 million short (75mb) sequence read pairs.<sup>33</sup> Raw sequence reads were aligned to the human reference (hg19) using the Burrows-Wheeler Aligner (BWA) (0.6.9) “aln” algorithm after hard trimming to 50bp. Duplicates were flagged using the Picard suite of tools. Post processing of the aligned data was done using the (GATK v1.6–19) including local realignment and base quality recalibration. Variant detection was done using the UnifiedGenotyper from GATK and called collectively to a multi-sample variant call format (VCF) file. Low quality sites were flagged using the VariantFiltrationWalker in agreement with the GATK BestPractices using filter thresholds  $Qual < 50$ ,  $QD < 5$ , and  $AB > 0.75$ .

### mRNA Quantitation

Real-time quantitative RT-PCR (qPCR) was performed in HEK cells expressing SCN5A after 24hr exposure to azithromycin or vehicle as described previously (Data Supplement).<sup>34, 35</sup>

### Protein Quantitation

Western analysis to quantitate SCN5A protein in HEK cells was performed as described (Data Supplement).<sup>35–37</sup> Both whole-cell lysate and biotinylated fraction were analyzed to quantitate total cellular and plasma membrane-bound protein, respectively.

### Azithromycin Plasma Concentrations

At 15min following IP injection (when electrophysiologic effects were maximal), animals were anesthetized with isoflurane and blood was harvested by cardiac puncture. During oral administration, animals were sacrificed at 90min (the time to maximal plasma concentration;<sup>31</sup>  $n=4$ ) or at 24hr (at trough or pre-dose;  $n=6$ ) following the last dose for measurement of azithromycin plasma concentration. Plasma was isolated for extraction and analysis of azithromycin concentration using LC/MS/MS as described.<sup>38</sup>

### Statistical Analysis

Data represented using a continuous variable were summarized using mean and standard error for each group. For group comparisons of a repeated measure, the non-parametric Wilcoxon signed-rank test was applied. For independent group comparisons, the non-

parametric Wilcoxon rank-sum test was used. Exact p values were calculated for these tests. For comparisons between multiple dose groups or time groups, p values were adjusted using the Bonferroni correction method. For each parameter of mouse ECG data, a linear regression with robust standard errors and consideration of mouse cluster analysis was also performed. The mean differences between dose groups and the confidence intervals were estimated. Two-sided nominal level of 0.05 was considered as statistically significant. Analyses were performed using R 3.2.4 (<https://www.R-project.org/>), Origin Pro 2016 (Origin Lab Corporation, Northampton MA 01060), and Microsoft Excel 2010.

## Results

### Case Report

The patient was a 24-year-old African American female with no prior past medical history who was treated for 5 days with azithromycin (Zithromycin Z-Pak) for an upper respiratory infection. She was taking no other medications or supplements. Within 24 hours after discontinuing azithromycin, she experienced recurrent episodes of syncope and presented to a local emergency department. Her ECG on admission was normal (Supplemental Figure 1). A rhythm strip obtained during a syncopal episode demonstrated rapid, polymorphic ventricular tachycardia in the setting of a normal QT interval (Figure 1). She remained off azithromycin, and the VT resolved over 3 days. A cardiac MRI was within normal limits. The patient received an ICD prior to discharge. Whole exome sequencing was performed, and there were no rare non-synonymous variants identified in genes previously associated with inherited arrhythmia syndromes.

### Acute Electrophysiologic Effects of Azithromycin in Conscious Mice

As an initial step to investigate the electrophysiologic effects of azithromycin *in vivo*, the drug was injected IP into conscious mice during continuous ECG monitoring. Within 15min, azithromycin produced diffuse, dose-dependent depressant effects on cardiac automaticity and conduction (Figure 2, Table 1), with reversible slowing of heart rate (Supplemental Figure 2), and significant increases in the PR, QRS, QT, and QTc intervals (Supplemental Table 1). Similar findings were observed following oral administration, with sinus slowing and an increase in all ECG intervals within 60min of dosing (Supplemental Figure 3, Supplemental Table 2) and to a lesser extent 24hr after dosing. These results are consistent with the effects of azithromycin overdose in humans, and they imply that acute administration of azithromycin blocks multiple depolarizing and repolarizing ionic currents in cardiomyocytes.

In separate groups of mice, plasma azithromycin concentrations were determined following IP injection (at 15min) and oral dosing (at 90min when plasma concentrations were maximal<sup>31</sup>, and at 24hr). Values were  $0.09 \pm 0.03 \mu\text{g/ml}$  and  $0.26 \pm 0.4 \mu\text{g/ml}$  after 50 and 100 mg/kg IP injection, respectively (n=3 each). For oral administration, plasma concentrations were  $0.12 \pm 0.01 \mu\text{g/ml}$  and  $0.07 \pm 0.01 \mu\text{g/ml}$  at 90min and 24h post dosing (n=4, 6, respectively). For comparison, peak plasma concentrations in humans are shown during chronic oral dosing with the 3 azithromycin regimens available commercially (Supplemental Table 3, from the product package insert). Thus, azithromycin concentrations resembling

those seen clinically were achieved during these experiments. However, the depressant ECG effects seen in the mouse are not observed clinically with oral administration in humans, demonstrating substantial inter-species pharmacokinetic differences.

### Acute Effects of Azithromycin on Cardiomyocyte Action Potentials

To further confirm these effects for cardiomyocytes, we examined the effects of azithromycin on HL-1 cells, a cultured cardiac cell line that displays spontaneous automaticity. Acute exposure caused slowing of beat rate, a reduction in the phase 0 upstroke slope, and prolonged repolarization (Table 2 and Supplemental Figure 4A–4C), consistent with the diffuse depressant effects observed *in vivo*.

### Reduction of SCN5A Currents with Acute Exposure

The QRS widening *in vivo* and reduced phase 0 upstroke in cardiomyocytes implied block of cardiac Na<sup>+</sup> current by azithromycin. In HEK cells expressing human SCN5A channels, azithromycin caused rapid block of I<sub>Na</sub>, with an IC<sub>50</sub> of ~110 μM, findings that were further confirmed in mouse ventricular myocytes (Figure 3A–3D, Table 3). Suppression of Na<sup>+</sup> current was accompanied by a depolarizing shift in the voltage dependence of channel activation and a hyperpolarizing shift in inactivation (Figure 3E and 3F, Table 3), changes that can account at least to some extent for the reduction in I<sub>Na</sub> observed.<sup>39</sup>

### Paradoxical Time-dependent Increase in Peak I<sub>Na</sub>

Recent studies have highlighted the importance of time-dependent effects of electrophysiologically-active agents on cardiac I<sub>Na</sub>.<sup>40, 41</sup> To determine whether such properties might also be present for azithromycin, we characterized Na<sup>+</sup> current in cells chronically exposed to the drug (for 24h), compared to control (vehicle-exposed) cells. Interestingly, under these conditions, peak SCN5A current density was increased at all test potentials examined, with up-regulation of nearly 2 fold at –20mV (Figure 4A–4B, Table 4). As for acute exposure, the voltage dependence of channel gating was also modulated (Figure 4C–4D, Table 4). However, in this case, these effects could not contribute to potentiation of cardiac I<sub>Na</sub>. These findings were replicated in HL-1 cardiomyocytes, with a substantial increase in peak Na<sup>+</sup> current and similar gating shifts upon chronic azithromycin exposure (Table 4, Supplemental Figure 5). Consistent with this effect, the phase 0 upstroke slope was increased in HL-1 cardiomyocyte action potentials under similar conditions (Table 2, Supplemental Figure 4D–4E).

To explore the mechanism of azithromycin-mediated potentiation of Na<sup>+</sup> current, experiments were performed using qPCR and Western analysis to determine if the drug altered the production of SCN5A mRNA, total cellular channel protein, or protein at the cell surface (using biotinylation). However, azithromycin had no effect on any of these properties for SCN5A (Supplemental Figure 6).

### Time-dependent Increase in Late I<sub>Na</sub>

Rarely, azithromycin causes drug-induced long QT syndrome. One potential mechanism is an increase in the Na<sup>+</sup> window current, defined by overlap of the activation and inactivation curves, or a window of potentials over which a fraction of Na<sup>+</sup> channels are activated but not

inactivated. However, azithromycin caused either no change or a reduction, rather than an increase, in the window current with acute and chronic exposure (Supplemental Figure 7).

Because an increase in late  $\text{Na}^+$  current can also prolong repolarization, we investigated the effects of azithromycin on this parameter using TTX subtraction in HEK cells expressing SCN5A (Figure 5A). Acute exposure to azithromycin had minimal effect on amplitude of late  $I_{\text{Na}}$  (Figure 5B and Table 3); however, chronic exposure for 24hr caused doubling of the late  $\text{Na}^+$  current (Figure 5A–5B, Table 4). Potentiation of late  $I_{\text{Na}}$  was greater than the increase in peak  $I_{\text{Na}}$ , illustrated by an increase in the ratio of these parameters (Supplemental Figure 8). The effects of chronic azithromycin exposure to increase both peak and late  $I_{\text{Na}}$  occurred at lower concentrations ( $\text{IC}_{50} = 40.9$  and  $62.2\mu\text{M}$ , respectively; Figure 5C–5D) than those causing acute  $I_{\text{Na}}$  block ( $\text{IC}_{50} = 110$ – $116\mu\text{M}$ ; Figure 3) implying greater clinical relevance during therapeutic dosing.

### Minimal Effects on the Rapid- and Slowly-activating Delayed Rectifier $\text{K}^+$ Currents

Most drugs prolong cardiac repolarization by blocking the delayed rectifier  $\text{K}^+$  current,  $I_{\text{Kr}}$ . In HEK cells expressing hERG,  $\text{K}^+$  currents displayed only mild block by azithromycin, with an  $\text{IC}_{50}$  of  $219\pm 21\mu\text{M}$  (Figure 6, Table 5). Similarly, there was minimal effect of the drug on the slowly-activating delayed rectifier,  $I_{\text{Ks}}$  (Figure 7, Table 5;  $\text{IC}_{50}=184\pm 12\mu\text{M}$ ). Given that these concentrations are 3–4 fold higher than that for potentiation of late  $I_{\text{Na}}$ , azithromycin-mediated QT prolongation most likely results from increase late  $\text{Na}^+$  current, rather than  $\text{K}^+$  channel block.

### Block of Cardiac Calcium Currents and $I_{\text{K1}}$

Because azithromycin slows sinus node automaticity and prolongs AV nodal conduction *in vivo*, we tested the hypothesis that the drug blocks cardiac  $\text{Ca}^{++}$  currents. Using rabbit ventricular myocytes, nimodipine-sensitive L-type  $\text{Ca}^{++}$  currents were suppressed by azithromycin ( $\text{IC}_{50}=67\pm 4\mu\text{M}$ ; Figure 8A–8B, Table 5), while mibefradil-sensitive T-type  $\text{Ca}^{++}$  currents were minimally affected ( $\text{IC}_{50}$  not determined; Figure 8C–8D, Table 5).

Azithromycin increased the maximal diastolic potential in HL-1 cells during both acute and chronic exposure (Table 2), implying an effect on the inward rectifier current  $I_{\text{K1}}$ . Indeed, for HEK cells expressing Kir2.1 and for HL-1 cells, azithromycin suppressed Kir and  $I_{\text{K1}}$  currents, respectively ( $\text{IC}_{50}=43.8\mu\text{M}$  for Kir2.1 currents; Table 5, Supplemental Figure 9).

## Discussion

Azithromycin is a widely prescribed macrolide antibiotic that has been linked to an increased risk of sudden cardiac death and cardiovascular death.<sup>11</sup> In contrast to other macrolides, torsades de pointes has been rarely reported for azithromycin.<sup>3–5, 7–9</sup> Thus, the cause of these adverse events has remained poorly defined, prompting the present investigation. As demonstrated by the case presented here, azithromycin can cause a unique, drug-mediated proarrhythmic syndrome characterized by rapid, polymorphic VT in the absence of QT prolongation or demonstrable cardiac structural abnormalities.<sup>6</sup> We found that chronic drug exposure markedly potentiates cardiac  $\text{Na}^+$  current, which would increase intracellular  $[\text{Na}^+]$  and subsequently promote dysregulation of intracellular  $[\text{Ca}^{++}]$ ,



providing a unifying mechanism for this unusual syndrome that likely contributes to azithromycin-mediated sudden cardiac death.

It is well recognized that conditions associated with intracellular  $\text{Na}^+$  loading, most notably digoxin therapy and ischemia, alter intracellular  $\text{Ca}^{++}$  homeostasis via the  $\text{Na}^+$ - $\text{Ca}^{++}$  exchanger activity, with removal of  $\text{Na}^+$  in exchange for  $\text{Ca}^{++}$ , leading to delayed after-depolarizations and triggered arrhythmias.<sup>32</sup> Abnormal intracellular  $\text{Ca}^{++}$  homeostasis due to SR  $\text{Ca}^{++}$  leak is the hallmark of CPVT, the clinical syndrome that most closely resembles this type of azithromycin proarrhythmia. Recent evidence further supporting the arrhythmogenic effects of cellular  $\text{Na}^+$  loading derives from a transgenic mouse model in which peak  $\text{Na}^+$  current was increased.<sup>42</sup> Mutations in *Scn1b*, encoding the  $\text{Na}^+$  channel  $\beta_1$  subunit, have been linked to inherited arrhythmia syndromes, including sudden infant death syndrome and unexplained death in epilepsy.<sup>43, 44</sup> Mice with cardiac-specific deletion of *Scn1b* demonstrated enhanced peak  $I_{\text{Na}}$ , delayed after-depolarizations, and polymorphic VT without APD prolongation, which was responsive to treatment with tetrodotoxin. Moreover, CPVT was recently linked to a gain-of-function mutation in *Scn5a* that increased  $\text{Na}^+$  influx by augmenting the  $\text{Na}^+$  channel window current.<sup>45</sup> Along with other studies,<sup>46, 47</sup> these data provide compelling evidence that a generalized increase in cardiac  $\text{Na}^+$  current is arrhythmogenic by dysregulating intracellular  $\text{Ca}^{++}$ , with clinical features exemplified by CPVT that mimic the unusual form of drug-mediated proarrhythmia described here.

Azithromycin can cause life-threatening arrhythmias by at least 2 other mechanisms, although these appear to be rare. First, cases of drug-induced long QT syndrome have been reported, but as noted above, documented torsades is unusual. Based on our results, potentiation of late  $I_{\text{Na}}$  by azithromycin appears to be responsible for this adverse effect, occurring at much lower concentrations than those required for  $\text{K}^+$  channel block. Drug-induced long QT syndrome is less common with azithromycin than with other drugs that also increase late  $I_{\text{Na}}$ , such as dofetilide.<sup>41</sup> This is likely because many of the compounds that increase late  $\text{Na}^+$  current also block  $I_{\text{Kr}}$  as well, and this is minimal with azithromycin. We speculate that concomitant block of cardiac  $\text{Ca}^{++}$  current by azithromycin might also provide an additional potential protective mechanism to prevent early afterdepolarizations and torsades.

Second, acute intravenous exposure<sup>14</sup> (in one case causing overdose<sup>15</sup>) can cause widespread depression of cardiac conduction, resulting in marked sinus bradycardia, slowing of AV nodal and infranodal conduction with heart block, and prolonged ventricular repolarization. For conscious mice and cardiomyocytes, we found that acute exposure to azithromycin had similar effects, with *in vitro* evidence of multi-ion channel block, providing a mechanistic basis for the electrophysiologic effects of acute toxicity. While these toxic effects have not been observed during oral dosing of azithromycin, we cannot rule out the participation of multi-ion channel block to drug-mediated sudden cardiac death. This is particularly true for acute  $\text{Na}^+$  channel block, as well as block of  $I_{\text{K1}}$ , which would elevate the myocyte resting potential leading to both enhanced automaticity and additional  $\text{Na}^+$  channel inactivation.

An important consideration is the range of azithromycin concentrations that we studied. Several oral preparations of azithromycin have been marketed and peak plasma concentrations during oral dosing range from ~0.4 to 1.1  $\mu\text{M}$  (Table 3 in the Data Supplement).<sup>48</sup> However, plasma concentrations are misleading, as the drug accumulates within cells, achieving concentrations approaching 900  $\mu\text{M}$  in leukocytes and pulmonary tissue (Supplemental Table 3<sup>48</sup>). A previous study by the pharmaceutical sponsor reported similar accumulation of the drug in cardiac cells for mice receiving oral azithromycin (200 mg/kg/d for 10 days), with ~30–220 fold increase in concentration compared to plasma.<sup>22</sup> Based on these data and known azithromycin plasma concentrations in patients, we investigated azithromycin concentrations of 0.1–1000  $\mu\text{M}$ , in order to account for intracellular accumulation. Interestingly, amitriptyline also accumulates in cardiomyocytes.<sup>49</sup> Intracellular concentrations were ~5 fold higher than extracellular concentrations, explaining the drug's higher potency in cardiomyocytes compared to RYR2 channels incorporated into lipid bilayers.

The mechanism for azithromycin-mediated potentiation of cardiac  $\text{Na}^+$  current remains unclear, as we found no evidence for increased production of *SCN5A* mRNA or total cellular protein, and there was no evidence for enhanced trafficking of channel protein to the cell surface. The alterations in channel gating, as well as the more selective increase in late  $I_{\text{Na}}$ , also argue against a nonspecific or generalized effect to increase  $\text{Na}^+$  channels at the membrane. We postulate that the increase in  $I_{\text{Na}}$  is mediated by effects that alter post-translational modification and/or protein-protein interactions, which could be complex.<sup>50</sup>

In conclusion, chronic exposure to azithromycin markedly potentiates cardiac  $\text{Na}^+$  current to promote intracellular  $\text{Na}^+$  loading, providing a unifying mechanistic basis for the distinct type of proarrhythmia seen with this drug. These findings imply that pre-clinical screening of new compounds should include examination of their pharmacologic effects on cardiac  $I_{\text{Na}}$  amplitude.

## Supplementary Material

Refer to Web version on PubMed Central for supplementary material.

## Acknowledgments

**Sources of Funding:** This work was supported by grants from the National Institutes of Health [HL108037, HL096844, HL049989, HL065962, and T32 GM007569] and the American Heart Association [16POST27250138]. K.B. is supported by NIGMS T32 GM07347 through the Vanderbilt Medical-Scientist Training Program and NHLBI F30HL127962.

## References

1. Roden DM. Clinical practice. Long-QT syndrome. *N Engl J Med*. 2008; 358:169–176. [PubMed: 18184962]
2. Owens RC Jr, Nolin TD. Antimicrobial-associated QT interval prolongation: Pointes of interest. *Clin Infect Dis*. 2006; 43:1603–1611. [PubMed: 17109296]
3. Arellano-Rodrigo E, Garcia A, Mont L, Roque M. Torsade de pointes and cardiorespiratory arrest induced by azithromycin in a patient with congenital long QT syndrome. *Med Clin (Barc)*. 2001; 117:118–119. [PubMed: 11459586]

4. Huang BH, Wu CH, Hsia CP, Yin CC. Azithromycin-induced torsade de pointes. *Pacing Clin Electrophysiol.* 2007; 30:1579–1582. [PubMed: 18070319]
5. Kezerashvili A, Khattak H, Barsky A, Nazari R, Fisher JD. Azithromycin as a cause of QT-interval prolongation and torsade de pointes in the absence of other known precipitating factors. *J Interv Card Electrophysiol.* 2007; 18:243–246. [PubMed: 17546486]
6. Kim MH, Berkowitz C, Trohman RG. Polymorphic ventricular tachycardia with a normal QT interval following azithromycin. *Pacing Clin Electrophysiol.* 2005; 28:1221–1222. [PubMed: 16359290]
7. Matsunaga N, Oki Y, Prigollini A. A case of QT-interval prolongation precipitated by azithromycin. *N Z Med J.* 2003; 116:U666. [PubMed: 14615808]
8. Russo V, Puzio G, Siniscalchi N. Azithromycin-induced QT prolongation in elderly patient. *Acta Biomed.* 2006; 77:30–32. [PubMed: 16856707]
9. Samarendra P, Kumari S, Evans SJ, Sacchi TJ, Navarro V. QT prolongation associated with azithromycin/amiodarone combination. *Pacing Clin Electrophysiol.* 2001; 24:1572–1574. [PubMed: 11707055]
10. Poluzzi E, Raschi E, Moretti U, De PF. Drug-induced torsades de pointes: data mining of the public version of the FDA Adverse Event Reporting System (AERS). *Pharmacoepidemiol Drug Saf.* 2009; 18:512–518. [PubMed: 19358226]
11. Ray WA, Murray KT, Hall K, Arbogast PG, Stein CM. Azithromycin and the risk of cardiovascular death. *N Engl J Med.* 2012; 366:1881–1890. [PubMed: 22591294]
12. Darbar D, Roden DM. Future of antiarrhythmic drugs. *Curr Opin Cardiol.* 2006; 21:361–367. [PubMed: 16755206]
13. Knollmann BC, Roden DM. A genetic framework for improving arrhythmia therapy. *Nature.* 2008; 451:929–936. [PubMed: 18288182]
14. Santos N, Oliveira M, Galrinho A, Oliveira JA, Ferreira L, Ferreira R. QT interval prolongation and extreme bradycardia after a single dose of azithromycin. *Rev Port Cardiol.* 2010; 29:139–142. [PubMed: 20391905]
15. Tilelli JA, Smith KM, Pettignano R. Life-threatening bradyarrhythmia after massive azithromycin overdose. *Pharmacotherapy.* 2006; 26:147–150. [PubMed: 16506357]
16. Roden DM. Cellular basis of drug-induced torsades de pointes. *Br J Pharmacol.* 2008; 154:1502–1507. [PubMed: 18552874]
17. Haverkamp W, Breithardt G, Camm AJ, Janse MJ, Rosen MR, Antzelevitch C, Escande D, Franz M, Malik M, Moss A, Shah R. The potential for QT prolongation and pro-arrhythmia by non-antiarrhythmic drugs: clinical and regulatory implications. Report on a Policy Conference of the European Society of Cardiology. *Cardiovasc Res.* 2000; 47:219–233. [PubMed: 10947683]
18. Fenichel RR, Malik M, Antzelevitch C, Sanguinetti M, Roden DM, Priori SG, Ruskin JN, Lipicky RJ, Cantilena LR. Drug-induced torsades de pointes and implications for drug development. *J Cardiovasc Electrophysiol.* 2004; 15:475–495. [PubMed: 15090000]
19. Webster G, Berul CI. Congenital long-QT syndromes: a clinical and genetic update from infancy through adulthood. *Trends Cardiovasc Med.* 2008; 18:216–224. [PubMed: 19185812]
20. Liu N, Colombi B, Raytcheva-Buono EV, Bloise R, Priori SG. Catecholaminergic polymorphic ventricular tachycardia. *Herz.* 2007; 32:212–217. [PubMed: 17497254]
21. Liu N, Rizzi N, Boveri L, Priori SG. Ryanodine receptor and calsequestrin in arrhythmogenesis: what we have learnt from genetic diseases and transgenic mice. *J Mol Cell Cardiol.* 2009; 46:149–159. [PubMed: 19027025]
22. Araujo FG, Shepard RM, Remington JS. In vivo activity of the macrolide antibiotics azithromycin, roxithromycin and spiramycin against *Toxoplasma gondii*. *Eur J Clin Microbiol Infect Dis.* 1991; 10:519–524. [PubMed: 1655433]
23. Panama BK, McLerie M, Lopatin AN. Heterogeneity of IK1 in the mouse heart. *Am J Physiol Heart Circ Physiol.* 2007; 293:H3558–H3567. [PubMed: 17890431]
24. Moyer BD, Loffing J, Schwiebert EM, Loffing-Cueni D, Halpin PA, Karlson KH, Ismailov II, Guggino WB, Langford GM, Stanton BA. Membrane trafficking of the cystic fibrosis gene product, cystic fibrosis transmembrane conductance regulator, tagged with green fluorescent

- protein in madin-darby canine kidney cells. *J Biol Chem.* 1998; 273:21759–21768. [PubMed: 9705313]
25. Zhou Z, Gong Q, Ye B, Fan Z, Makielski JC, Robertson GA, January CT. Properties of HERG channels stably expressed in HEK 293 cells studied at physiological temperature. *Biophys J.* 1998; 74:230–241. [PubMed: 9449325]
  26. Lundquist AL, Manderfield LJ, Vanoye CG, Rogers CS, Donahue BS, Chang PA, Drinkwater DC, Murray KT, George AL Jr. Expression of multiple KCNE genes in human heart may enable variable modulation of I(Ks). *J Mol Cell Cardiol.* 2005; 38:277–287. [PubMed: 15698834]
  27. Claycomb WC, Lanson NA Jr, Stallworth BS, Egeland DB, Delcarpio JB, Bahinski A, Izzo NJ Jr. HL-1 cells: A cardiac muscle cell line that contracts and retains phenotypic characteristics of the adult cardiomyocyte. *Proc Natl Acad Sci USA.* 1998; 95:2979–2984. [PubMed: 9501201]
  28. Yang Z, Murray KT. Ionic mechanisms of pacemaker activity in spontaneously contracting atrial HL-1 cells. *J Cardiovasc Pharmacol.* 2011; 57:28–36. [PubMed: 20881602]
  29. Bassani JW, Bassani RA, Bers DM. Calibration of indo-1 and resting intracellular [Ca]<sub>i</sub> in intact rabbit cardiac myocytes. *Biophys J.* 1995; 68:1453–1460. [PubMed: 7787031]
  30. Dzhura I, Wu Y, Colbran R, Balsler J, Anderson M. Calmodulin kinase determines calcium-dependent facilitation of L-type calcium channels. *Nature Cell Biol.* 2000; 2:173–177. [PubMed: 10707089]
  31. Girard AE, Girard D, English AR, Gootz TD, Cimochowski CR, Faiella JA, Haskell SL, Retsema JA. Pharmacokinetic and in vivo studies with azithromycin (CP-62,993), a new macrolide with an extended half-life and excellent tissue distribution. *Antimicrob Agents Chemother.* 1987; 31:1948–1954. [PubMed: 2830841]
  32. Mitchell GF, Jeron A, Koren G. Measurement of heart rate and Q-T interval in the conscious mouse. *Am J Physiol.* 1998; 274:H747–H751. [PubMed: 9530184]
  33. Weeke P, Mosley JD, Hanna D, Delaney JT, Shaffer C, Wells QS, Van DS, Karnes JH, Ingram C, Guo Y, Shyr Y, Norris K, Kannankeril PJ, Ramirez AH, Smith JD, Mardis ER, Nickerson D, George AL Jr, Roden DM. Exome sequencing implicates an increased burden of rare potassium channel variants in the risk of drug-induced long QT interval syndrome. *J Am Coll Cardiol.* 2014; 63:1430–1437. [PubMed: 24561134]
  34. Mace LC, Yermalitskaya LV, Yi Y, Yang Z, Morgan AM, Murray KT. Transcriptional remodeling of rapidly stimulated HL-1 atrial myocytes exhibits concordance with human atrial fibrillation. *J Mol Cell Cardiol.* 2009; 47:485–492. [PubMed: 19615375]
  35. Watanabe H, Yang T, Stroud DM, Lowe JS, Harris L, Atack TC, Wang DW, Hipkens SB, Leake B, Hall L, Kupersmidt S, Chopra N, Magnuson MA, Tanabe N, Knollmann BC, George AL Jr, Roden DM. Striking in vivo phenotype of a disease-associated human SCN5A mutation producing minimal changes in vitro. *Circulation.* 2011; 124:1001–1011. [PubMed: 21824921]
  36. Hallaq H, Yang Z, Viswanathan PC, Fukuda K, Shen W, Wang DW, Wells KS, Zhou J, Yi J, Murray KT. Quantitation of protein kinase A-mediated trafficking of cardiac sodium channels in living cells. *Cardiovasc Res.* 2006; 72:250–261. [PubMed: 16973141]
  37. Kupersmidt S, Yang T, Chanthaphaychith S, Wang Z, Towbin JA, Roden DM. Defective human Ether-a-go-go-related gene trafficking linked to an endoplasmic reticulum retention signal in the C terminus. *J Biol Chem.* 2002; 277:27442–27448. [PubMed: 12021266]
  38. Zur G, Soback S, Weiss Y, Perry E, Lavy E, Britzi M. Azithromycin pharmacokinetics in the serum and its distribution to the skin in healthy dogs and dogs with pyoderma. *Vet J.* 2014; 200:122–126. [PubMed: 24472431]
  39. Wilde AA, Brugada R. Phenotypical manifestations of mutations in the genes encoding subunits of the cardiac sodium channel. *Circ Res.* 2011; 108:884–897. [PubMed: 21454796]
  40. Lu Z, Wu CY, Jiang YP, Ballou LM, Clausen C, Cohen IS, Lin RZ. Suppression of phosphoinositide 3-kinase signaling and alteration of multiple ion currents in drug-induced long QT syndrome. *Sci Transl Med.* 2012; 4:131ra50.
  41. Yang T, Chun YW, Stroud DM, Mosley JD, Knollmann BC, Hong C, Roden DM. Screening for acute IKr block is insufficient to detect torsades de pointes liability: role of late sodium current. *Circulation.* 2014; 130:224–234. [PubMed: 24895457]

42. Lin X, O'Malley H, Chen C, Auerbach D, Foster M, Shekhar A, Zhang M, Coetzee W, Jalife J, Fishman GI, Isom L, Delmar M. Scn1b deletion leads to increased tetrodotoxin-sensitive sodium current, altered intracellular calcium homeostasis and arrhythmias in murine hearts. *J Physiol.* 2015; 593:1389–1407. [PubMed: 25772295]
43. Adsit GS, Vaidyanathan R, Galler CM, Kyle JW, Makielski JC. Channelopathies from mutations in the cardiac sodium channel protein complex. *J Mol Cell Cardiol.* 2013; 61:34–43. [PubMed: 23557754]
44. Dravet C. The core Dravet syndrome phenotype. *Epilepsia.* 2011; 52:3–9.
45. Swan H, Amarouch MY, Leinonen J, Marjamaa A, Kucera JP, Laitinen-Forsblom PJ, Lahtinen AM, Palotie A, Kontula K, Toivonen L, Abriel H, Widen E. Gain-of-function mutation of the SCN5A gene causes exercise-induced polymorphic ventricular arrhythmias. *Circ Cardiovasc Genet.* 2014; 7:771–781. [PubMed: 25210054]
46. Despa S, Bers DM. Na<sup>+</sup> transport in the normal and failing heart - remember the balance. *J Mol Cell Cardiol.* 2013; 61:2–10. [PubMed: 23608603]
47. Clancy CE, Chen-Izu Y, Bers DM, Belardinelli L, Boyden PA, Csernoch L, Despa S, Fermini B, Hool LC, Izu L, Kass RS, Lederer WJ, Louch WE, Maack C, Matiazzi A, Qu Z, Rajamani S, Ripinger CM, Sejersted OM, O'Rourke B, Weiss JN, Varro A, Zaza A. Deranged sodium to sudden death. *J Physiol.* 2015; 593:1331–1345. [PubMed: 25772289]
48. Zmax Package Insert. 2010.
49. Chopra N, Laver D, Davies SS, Knollmann BC. Amitriptyline activates cardiac ryanodine channels and causes spontaneous sarcoplasmic reticulum calcium release. *Mol Pharmacol.* 2009; 75:183–195. [PubMed: 18845675]
50. Rook MB, Evers MM, Vos MA, Bierhuizen MF. Biology of cardiac sodium channel Nav1.5 expression. *Cardiovasc Res.* 2012; 93:12–23. [PubMed: 21937582]

**WHAT IS KNOWN**

- The commonly used antibiotic azithromycin increases risk of cardiovascular and sudden cardiac death, but the underlying mechanisms are unclear.
- While torsades de pointes is rare, case reports indicate that azithromycin can also cause a novel proarrhythmic syndrome, characterized by polymorphic ventricular tachycardia in the setting of a normal QT interval.

**WHAT THE STUDY ADDS**

- Acutely, azithromycin causes diffuse depression of the cardiac conduction system and ion channel block, reminiscent of azithromycin overdose in humans.
- Chronically, the drug markedly potentiates cardiac sodium current to promote intracellular sodium loading, a condition associated with intracellular calcium overload and polymorphic ventricular tachycardia.
- These findings provide a unifying mechanistic basis for the novel form of proarrhythmia seen with azithromycin, which likely contributes to the increased risk of sudden cardiac death seen with this antibiotic.

**RHYTHM SHEET**

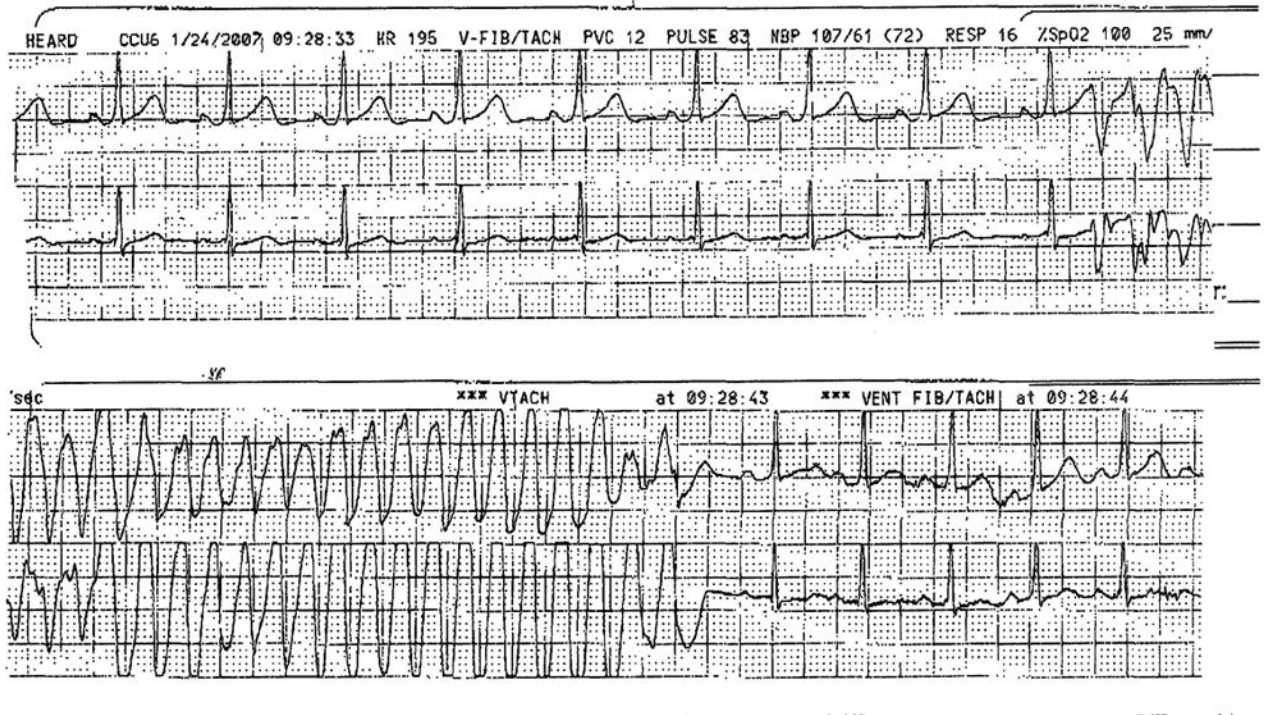


**Figure 1.** Azithromycin-induced polymorphic VT in a 24 year old female with no structural heart disease and a normal ECG. The arrhythmias resolved with stopping the drug.

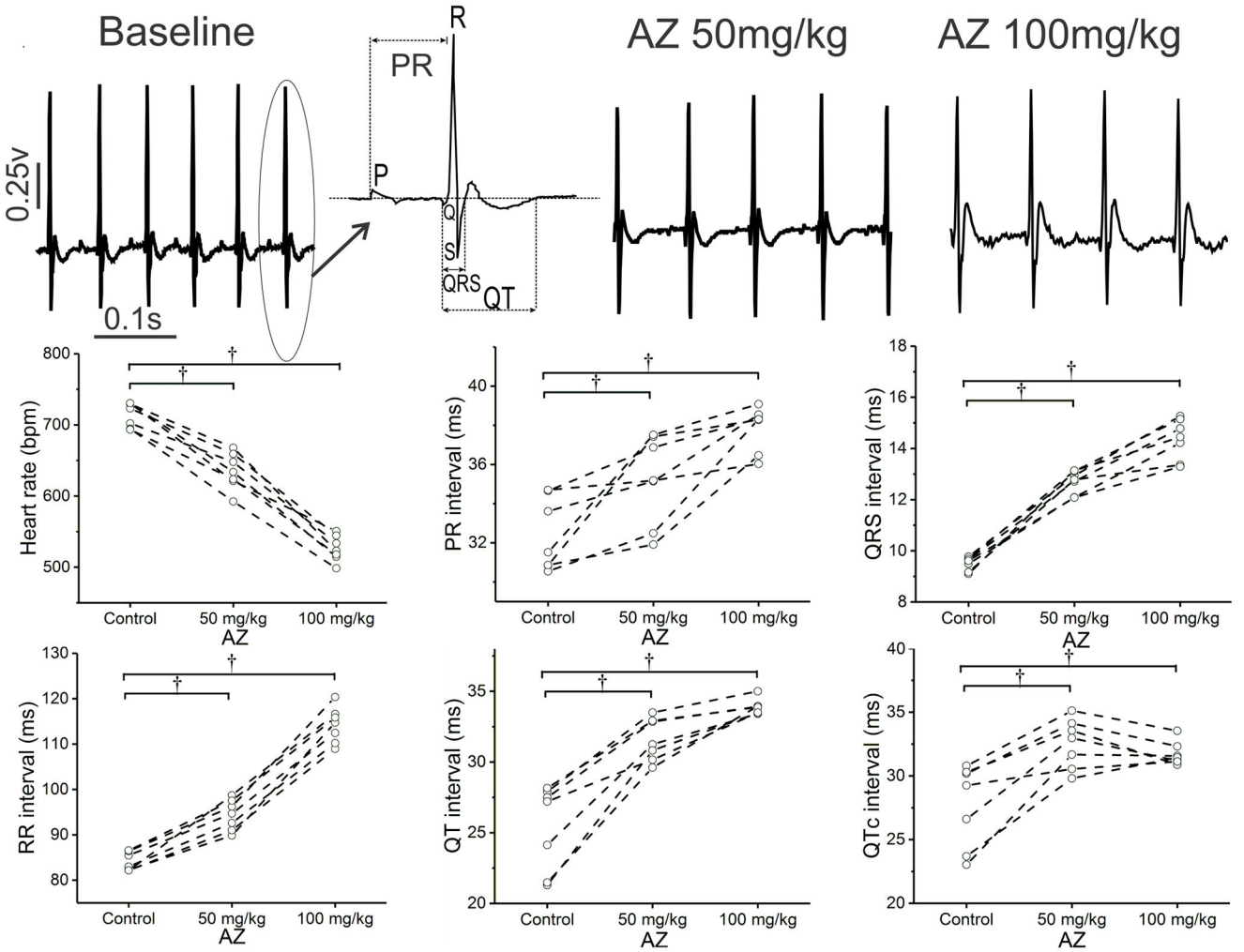


**Figure 2.** Effects of IP azithromycin (AZ) on the electrocardiogram of conscious adult mice. Mice received intraperitoneal injection of AZ (50 mg/kg, followed in 60 min by 100 mg/kg). Representative ECG tracings (and interval measurements) are shown in the upper panel, with parameter data for the group shown below (n=7). With both doses of AZ, heart rate declined, along with an increase in the PR, QRS, and QT/QTc intervals.



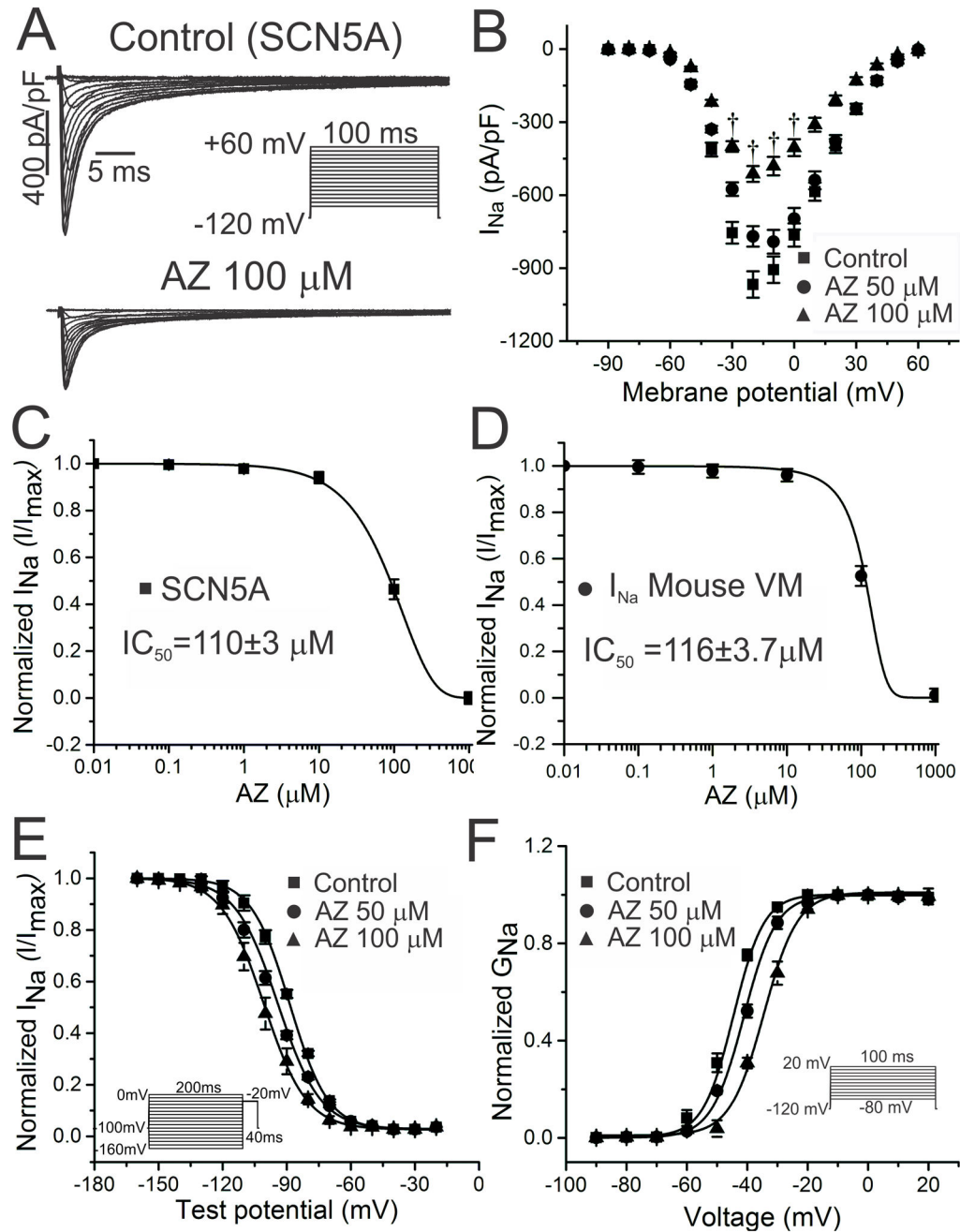


**Figure 3.** Concentration-dependent block of human and mouse cardiac Na<sup>+</sup> currents with acute AZ exposure. **A** and **B**. In HEK cells expressing human SCN5A, acute exposure to AZ significantly reduced I<sub>Na</sub> (from  $-967 \pm 54$  to  $-769 \pm 49$  and  $-512 \pm 38$  pA/pF for AZ 50 and 100  $\mu$ M, respectively, at  $-20$  mV [n=18, 14];  $\dagger P < 0.01$ ; representative current tracings in **A** and current-voltage plot of summary data in **B**). **C** and **D**. The concentration-response curve demonstrated an IC<sub>50</sub> of  $110 \pm 3 \mu$ M for SCN5A currents (**C**; n=6 for each concentration), with similar results obtained using mouse ventricular myocytes (**D**; VM; IC<sub>50</sub>  $116 \pm 4 \mu$ M; n=5 for each concentration). **E** and **F**. Using the voltage clamp protocols shown in the insets,

normalized steady-state inactivation (**E**) and activation (**F**) curves for SCN5A were generated and fit with a Boltzmann function. AZ caused small but significant shifts in the hyperpolarizing and depolarizing directions, respectively (n=14–32; <sup>†</sup>P<0.01 for AZ 100μM in **E** and **F**).

Author Manuscript

Author Manuscript

Author Manuscript

Author Manuscript

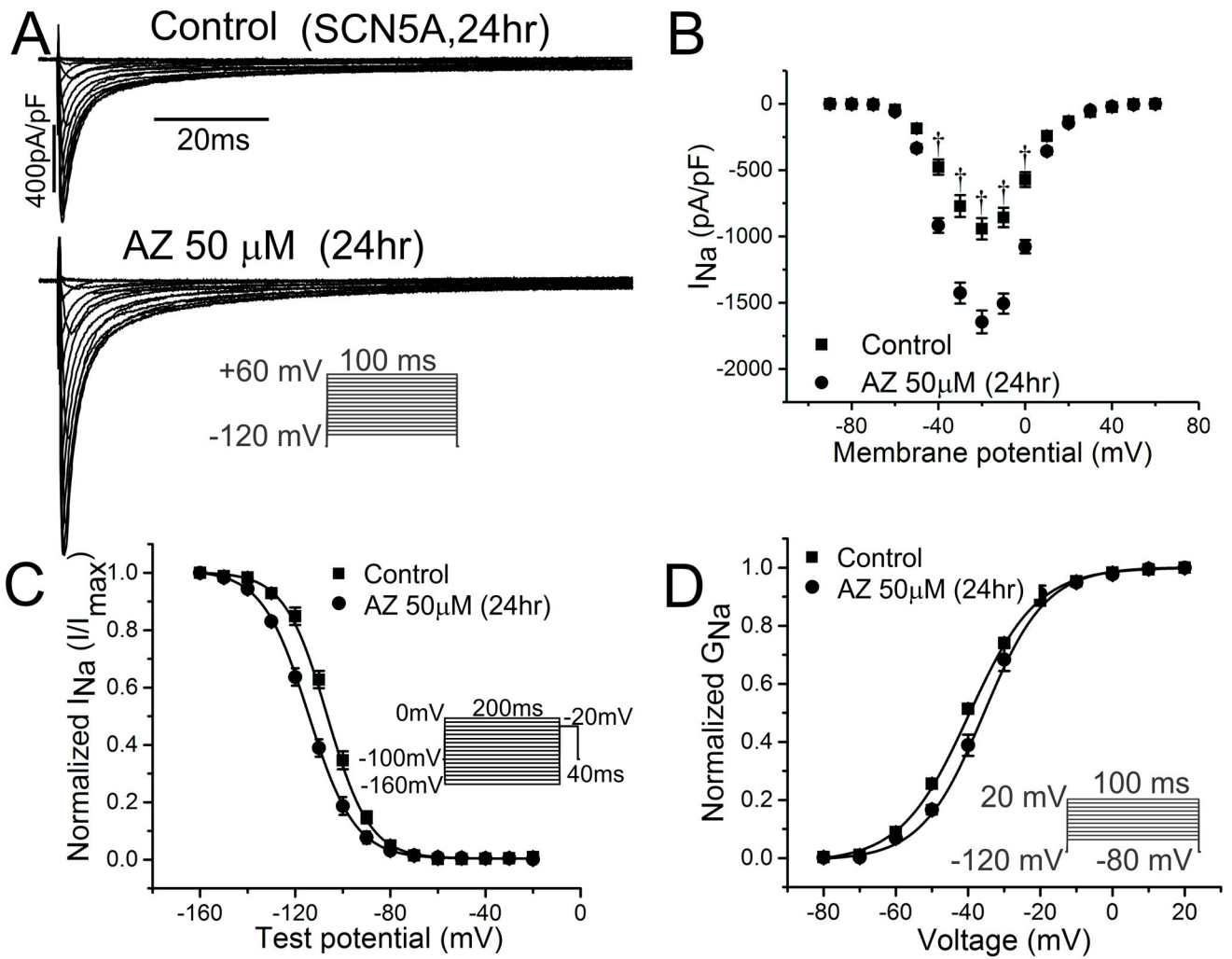


**Figure 4.** Increased peak Na<sup>+</sup> current with chronic AZ exposure. **A** and **B.** For SCN5A currents in HEK cells, incubation with AZ (50 $\mu$ M) for 24 hr significantly increased  $I_{Na}$  (from  $-942\pm 80$  pA/pF to  $-1644\pm 76$  pA/pF at  $-20$  mV;  $n=13$  each;  $^{\dagger}P<0.01$ ). **C** and **D.** In the same preparation, similar shifts were observed in the steady-state inactivation and activation curves, as those seen with acute exposure (for inactivation,  $-106.6\pm 1.2$  mV to  $-119.9\pm 1.2$  mV for control and AZ 50 $\mu$ M, respectively; for activation,  $-41.0\pm 2$  mV to  $-35.3\pm 1$  mV;  $n=14$  and  $*P<0.05$  for both).

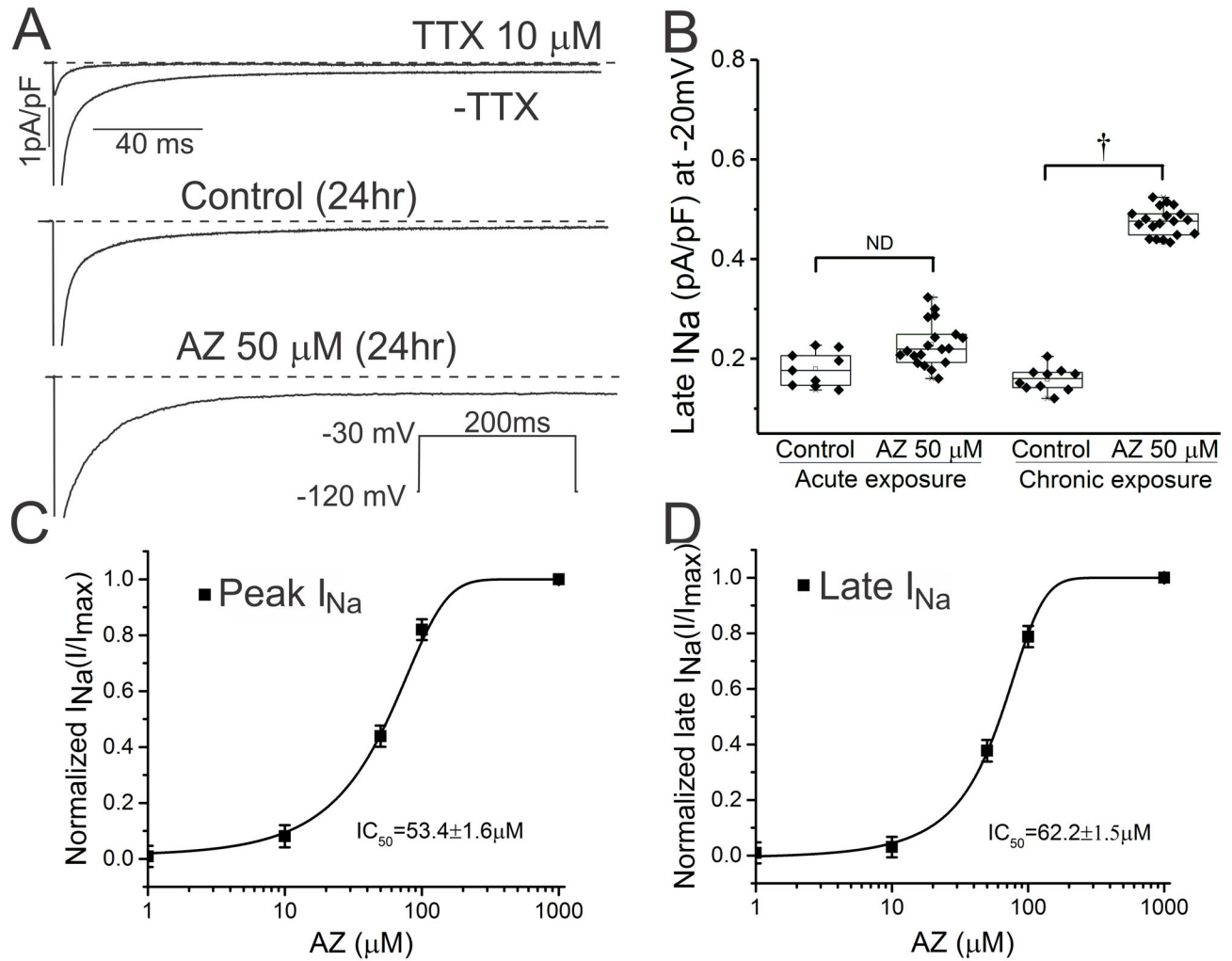


**Figure 5.** Time- and concentration-dependent increases in late and peak  $I_{\text{Na}}$ . **A.** For SCN5A currents, examples of tetrodotoxin-sensitive  $\text{Na}^+$  current (top panel) are shown in the absence (control; middle panel) and presence of 24 hr incubation with AZ (50 $\mu\text{M}$ ; bottom panel). **B.** Summary data demonstrate a significant increase in late  $I_{\text{Na}}$  (from  $0.18\pm 0.02$  pA/pF to  $0.48\pm 0.03$  pA/pF;  $n=6$ ;  $^{\dagger}P<0.01$ ) with chronic (24 hr) but not acute exposure. **C** and **D.** The concentration-response relationships for the increase in peak (**C**) and late (**D**) SCN5A currents following a 24hr exposure to azithromycin are illustrated.

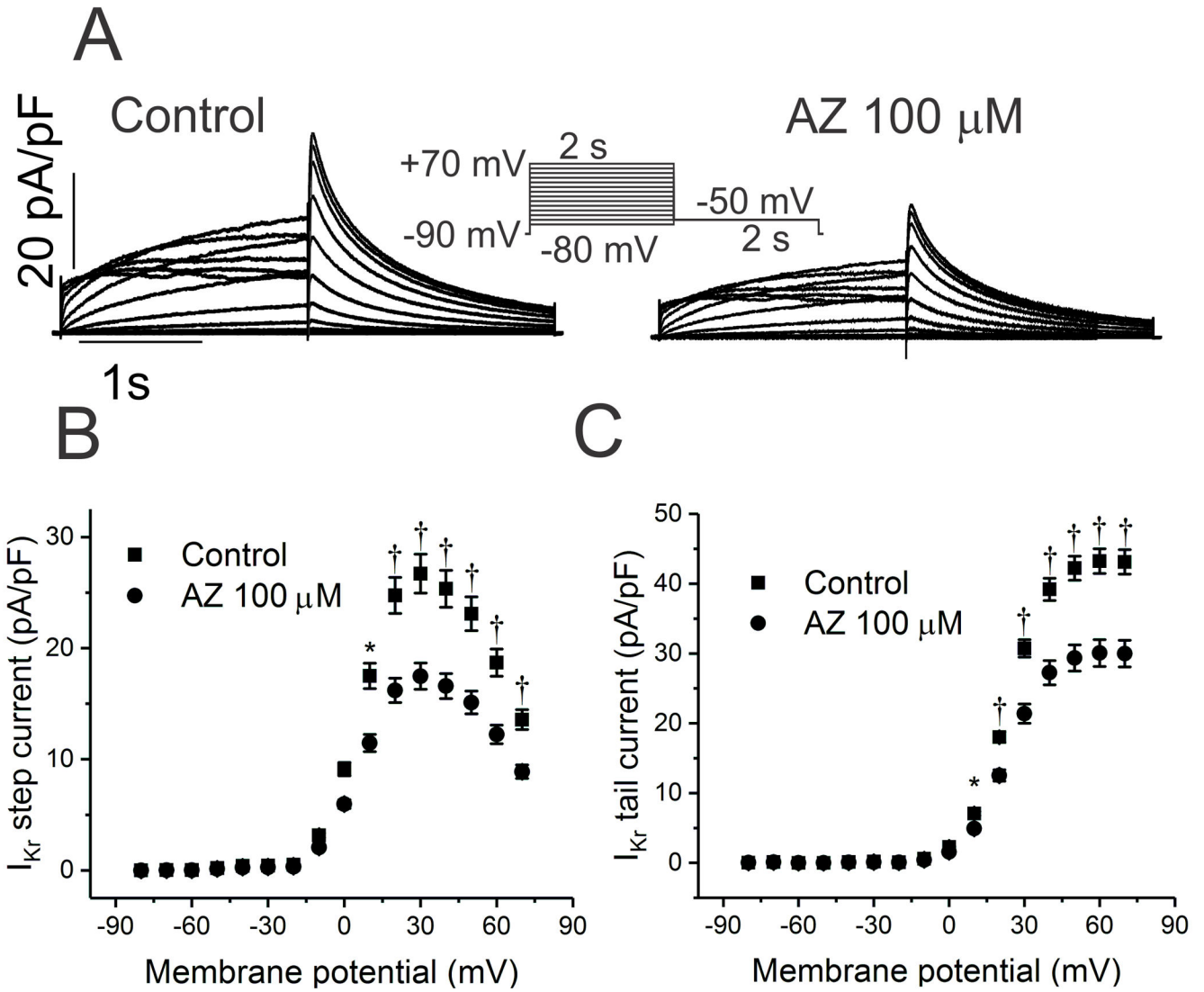


**Figure 6.** Effects of AZ on hERG currents ( $I_{Kr}$ ). **A.** In HEK cells expressing human KCNH2 (hERG),  $K^+$  currents were recorded in the absence and presence of AZ 100  $\mu$ M. **B** and **C.** Current-voltage relationships are shown for steady-state (**B**) and tail (**C**) current before and following acute exposure to AZ, with a reduction of 34 and 30% at +60 mV, respectively (n=15;  $IC_{50}$  219 $\pm$ 21 $\mu$ M; †P<0.01).

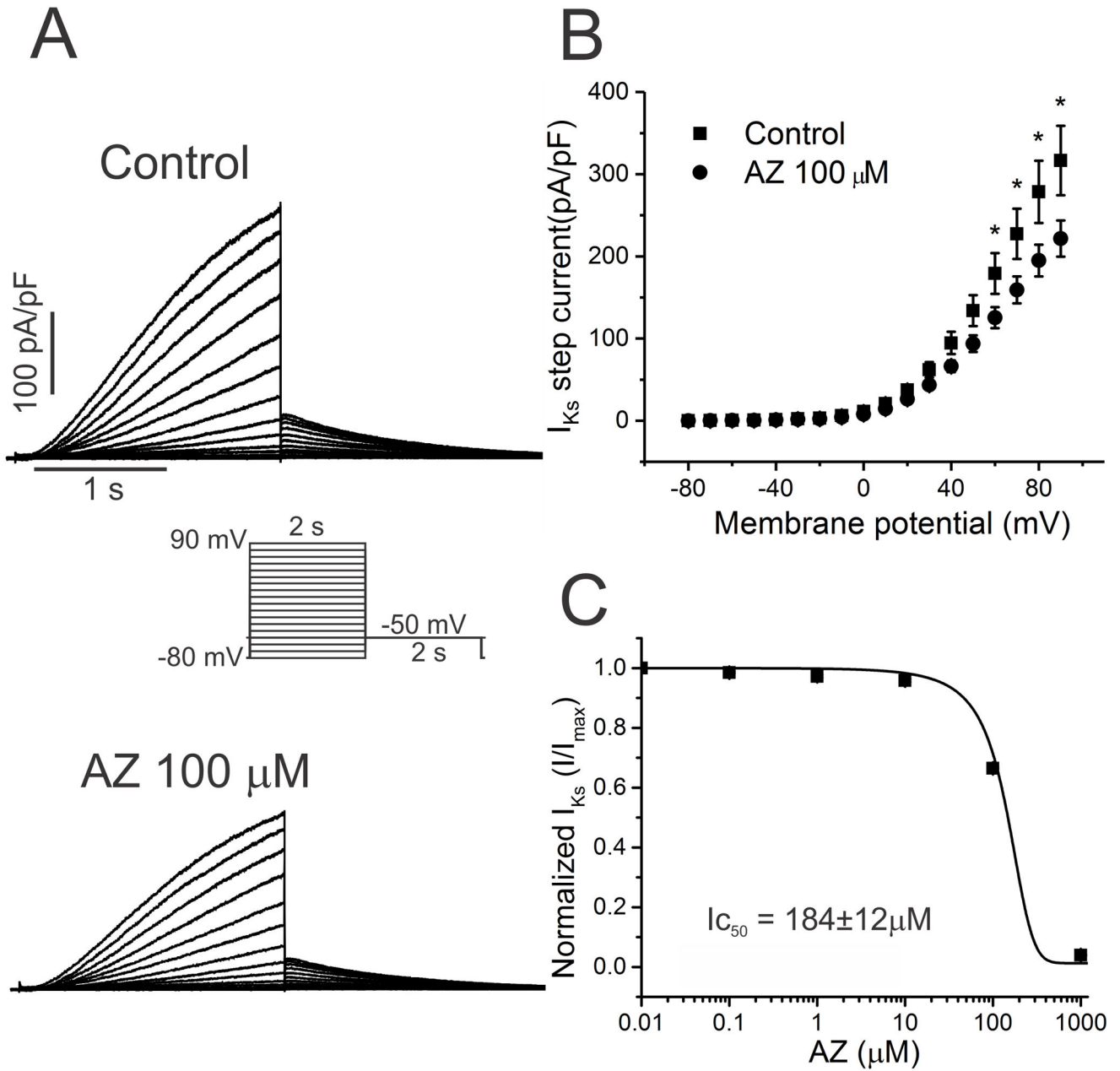


**Figure 7.** Minimal reduction in  $I_{Ks}$  current. **A.** In CHO cells stably expressing KCNQ1 and KCNE1,  $K^+$  currents were recorded using the voltage clamp protocol shown in the inset before and following acute exposure to AZ 100 $\mu$ M.  $I_{Ks}$  steady-state current was suppressed by 30% at +80 mV (n=12; \*P<0.05). **B.** Current-voltage plot of tail current demonstrated a 30% reduction at +80 mV (n=12; \*P<0.05). **C.** The concentration-response curve demonstrated an  $IC_{50}$  of 184 $\pm$ 12 $\mu$ M.

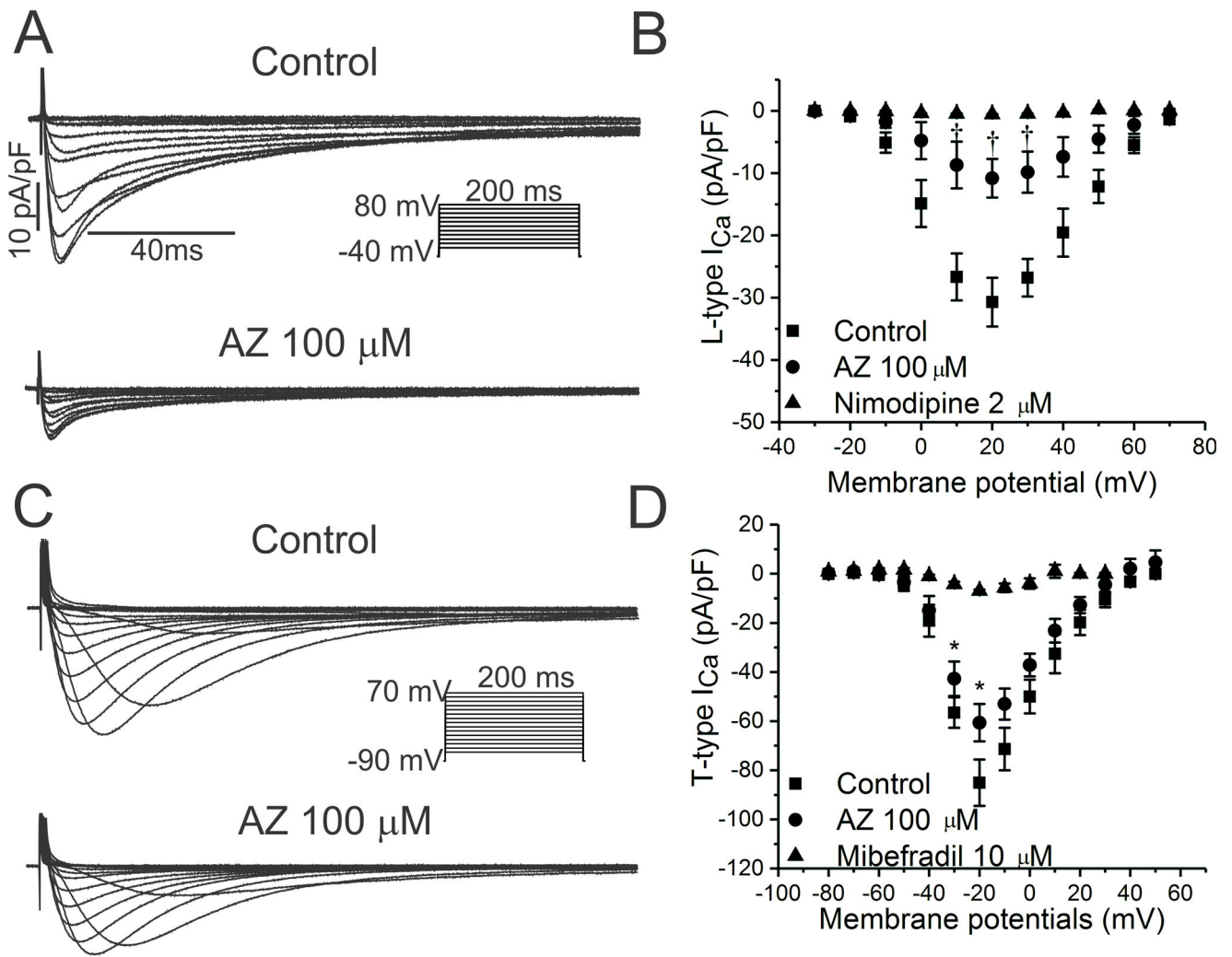


**Figure 8.** Effects of AZ on  $Ca^{++}$  currents in rabbit ventricular myocytes. **A** and **B**. Families of currents and peak current-voltage relationships are illustrated for nimodipine-sensitive  $Ca^{++}$  currents, indicative of  $I_{Ca-L}$ , before and following acute exposure to AZ 100  $\mu$ M, with a 65% reduction at +20 mV ( $n=7$ ;  $\dagger P<0.01$ ;  $IC_{50}$   $67\pm 4\mu$ M). **C** and **D**. Similar results are shown for mibefradil-sensitive  $Ca^{++}$  currents representing  $I_{Ca-T}$ , with 29% suppression at -20 mV ( $n=8$ ;  $*P<0.05$ ).

**Table 1**

Summary data of azithromycin effects on the ECG of conscious mice

|             | Heart rate (bpm)   | PR (ms)               | QRS (ms)              | QT (ms)               | QTc (ms)              |
|-------------|--------------------|-----------------------|-----------------------|-----------------------|-----------------------|
| Control     | 715±7              | 32.4±0.7              | 9.5±0.1               | 25.4±1.2              | 27.7±1.2              |
| AZ 50mg/kg  | 637±8 <sup>‡</sup> | 35.2±0.9 <sup>*</sup> | 12.7±0.2 <sup>‡</sup> | 31.6±0.6 <sup>‡</sup> | 32.5±0.7 <sup>‡</sup> |
| AZ 100mg/kg | 526±7 <sup>‡</sup> | 37.9±0.4 <sup>‡</sup> | 14.4±0.3 <sup>‡</sup> | 33.9±0.2 <sup>‡</sup> | 31.7±0.4 <sup>*</sup> |

Wilcoxon Signed Rank Test, Normalized Bazett:  $QTc = QT / (RR/100)^{1/2}$

N=7 mice;

<sup>\*</sup> P<0.05;

<sup>‡</sup> P<0.01



**Table 2**

Effects of azithromycin on action potentials

|                          |      | CL (ms)            | Peak (mV)         | MDP (mV)           | DDT (ms)          | Phase 0 slope (mV/ms) | APD <sub>100</sub> (ms) | APD <sub>90</sub> (ms) | Beat rate (bpm)    |
|--------------------------|------|--------------------|-------------------|--------------------|-------------------|-----------------------|-------------------------|------------------------|--------------------|
| <b>Acute (n=14)</b>      |      |                    |                   |                    |                   |                       |                         |                        |                    |
| <b>Control</b>           | Mean | 308.3              | 107.7             | -63.8              | 19.6              | 2.45                  | 288.6                   | 277.0                  | 194.9              |
|                          | SE   | 2.9                | 1.5               | 0.8                | 1.1               | 0.13                  | 2.8                     | 2.8                    | 1.8                |
| <b>AZ 100µM</b>          | Mean | 353.7 <sup>‡</sup> | 89.2 <sup>‡</sup> | -59.1 <sup>‡</sup> | 39.6 <sup>*</sup> | 1.18 <sup>*</sup>     | 314.1 <sup>‡</sup>      | 299.9 <sup>‡</sup>     | 169.9 <sup>‡</sup> |
|                          | SE   | 3.7                | 1.8               | 1.0                | 2.4               | 0.05                  | 4.1                     | 4.1                    | 1.8                |
| <b>Chronic (n=8)</b>     |      |                    |                   |                    |                   |                       |                         |                        |                    |
| <b>Control</b>           | Mean | 291.1              | 101.0             | -63.2              | 18.8              | 2.5                   | 272.3                   | 256.4                  | 207.5              |
|                          | SE   | 8.9                | 2.1               | 0.5                | 0.8               | 0.1                   | 8.3                     | 8.1                    | 11.1               |
| <b>AZ 100µM for 24hr</b> | Mean | 216.7 <sup>‡</sup> | 99.5              | -60.6 <sup>‡</sup> | 15.1 <sup>*</sup> | 4.0 <sup>*</sup>      | 201.6 <sup>‡</sup>      | 185.5 <sup>‡</sup>     | 285.0 <sup>‡</sup> |
|                          | SE   | 13.9               | 1.2               | 0.3                | 1.2               | 0.6                   | 12.9                    | 12.8                   | 13.4               |

Wilcoxon Signed Rank Test;

\* P<0.05;

<sup>‡</sup> P<0.01

AZ is Azithromycin; CL is cycle length; MDP is maximum diastolic potential; DDT is diastolic depolarization time; APD<sub>100</sub> is action potential duration at 100% of repolarization; APD<sub>90</sub> is action potential duration at 90% of repolarization; bpm is beats per minute.

Acute effects of azithromycin on SCN5A currents

**Table 3**

|                 | Peak $I_{Na}$ (n=14-18) |                      | Activation (n=14-32)    |         | Inactivation (n=14-32)  |         | Late $I_{Na}$ (n=12-16) |           |
|-----------------|-------------------------|----------------------|-------------------------|---------|-------------------------|---------|-------------------------|-----------|
|                 | pA/pF                   | $V_{1/2}$ mV         | $V_{1/2}$ mV            | k       | $V_{1/2}$ mV            | k       | k                       | pA/pF     |
| <b>CTL</b>      | -967±54                 | -44.6±1              | -88.6±0.6               | 5.0±0.5 | -88.6±0.6               | 7.9±0.1 | 0.17±0.02               | 0.17±0.02 |
| <b>AZ 50µM</b>  | -769±49                 | -41.1±1              | -94.2±0.6               | 5.3±0.3 | -94.2±0.6               | 9.9±0.2 | 0.23±0.02               | 0.23±0.02 |
| <b>AZ 100µM</b> | -512±38 <sup>†</sup>    | -34.5±1 <sup>†</sup> | -100.8±0.6 <sup>†</sup> | 5.6±0.3 | -100.8±0.6 <sup>†</sup> | 9.9±0.3 | -                       | -         |

Wilcoxon Signed Rank Test; k=slope factor;

<sup>†</sup>P<0.01

Chronic (24 hr) exposure of SCN5A currents to azithromycin

Table 4

|                        | Peak $I_{Na}$         |                      | Activation              |       | Inactivation |          | Late $I_{Na}$          |  |
|------------------------|-----------------------|----------------------|-------------------------|-------|--------------|----------|------------------------|--|
|                        | pA/pF                 | $V_{1/2}$ mV         | $V_{1/2}$ mV            | k     | $V_{1/2}$ mV | k        | pA/pF                  |  |
| <b>CTL (SCN5A)</b>     | -942±80               | -41.0±2              | -106.6±1.2              | 9.7±1 | 9.1±0.4      | 9.1±0.4  | 0.18±0.02              |  |
| <b>AZ 50µM</b>         | -1644±76 <sup>‡</sup> | -35.3±1 <sup>*</sup> | -119.9±1.2 <sup>*</sup> | 8.4±1 | 9.5±0.4      | 9.5±0.4  | 0.48±0.03 <sup>‡</sup> |  |
| <b>IC<sub>50</sub></b> | 53.3±1.6µM            |                      |                         |       |              |          | 62.2±1.5µM             |  |
| <b>CTL (HL-1cells)</b> | -81±19                | -49.8±1              | -93.8±1.3               | 8.1±1 | 9.5±0.4      | 9.5±0.4  | 0.21±0.02              |  |
| <b>AZ 50µM</b>         | -135±22 <sup>‡</sup>  | -47.6±1 <sup>*</sup> | -98.6±1.4 <sup>*</sup>  | 7.9±1 | 10.6±0.4     | 10.6±0.4 | 0.49±0.02 <sup>‡</sup> |  |

Wilcoxon Rank-sum Test; k=slope factor;

<sup>\*</sup> P<0.05;

<sup>‡</sup> P<0.01

**Table 5**

Acute effects of azithromycin on multiple ionic currents

| n                           | I <sub>Na</sub> (pA/pF) |                     | I <sub>Kr</sub> (pA/pF) |                       | I <sub>Ks</sub> (pA/pF) |                    | L-type I <sub>Ca</sub> (pA/pF) |                      | T-type I <sub>Ca</sub> (pA/pF) |                      | I <sub>K1</sub> (pA/pF) |                      |
|-----------------------------|-------------------------|---------------------|-------------------------|-----------------------|-------------------------|--------------------|--------------------------------|----------------------|--------------------------------|----------------------|-------------------------|----------------------|
|                             | Peak                    | SS                  | Tail                    | Tail                  | SS                      | Tail               | Peak                           | Peak                 | Peak                           | Peak                 | Peak                    | Peak                 |
| <b>Control</b>              | -967±54                 | 26.8±3              | 43.0±4                  | 316.7±42              | 49.6±3                  | -31±6              | -85.1±19                       | -79.5±6              | -85.1±19                       | -79.5±6              | -79.5±6                 | -79.5±6              |
| <b>AZ 100µM</b>             | -512±38 <sup>†</sup>    | 17.6±2 <sup>†</sup> | 30.1±4 <sup>†</sup>     | 221.6±22 <sup>*</sup> | 34.6±2 <sup>*</sup>     | -11±2 <sup>†</sup> | -60.6±16 <sup>*</sup>          | -27.2±6 <sup>†</sup> | -60.6±16 <sup>*</sup>          | -27.2±6 <sup>†</sup> | -27.2±6 <sup>†</sup>    | -27.2±6 <sup>†</sup> |
| <b>% inhibition</b>         | 47                      | 34                  | 30                      | 30                    | 30                      | 65                 | 29                             | 66                   | 29                             | 66                   | 66                      | 66                   |
| <b>IC<sub>50</sub> (µM)</b> | 110±3                   | 219±21              | 184±12                  | 66.5±4                | 66.5±4                  | 66.5±4             | 66.5±4                         | 43.8±3.2             | 66.5±4                         | 66.5±4               | 43.8±3.2                | 43.8±3.2             |

Wilcoxon Signed Rank Test;

\* P<0.05;

<sup>†</sup>P<0.01;

Peak is peak current; SS is steady-state current; Tail is tail current